Ultrasound in Med. & Biol., Vol. 42, No. 6, pp. 1412–1418, 2016

Printed in the USA
0301-5629
http://dx.doi.org/10.1016/j.ultrasmedbio.2016.01.005

● *Technical Note*

ANALYSIS OF THE UNCERTAINTY IN MICROBUBBLE CHARACTERIZATION

Caroline Harfield,* Christopher R. Fury,†‡ Gianluca Memoli,† Philip Jones,‡ Nick Ovenden,§ and Eleanor Stride*

*Institute of Biomedical Engineering, Department of Engineering Science, Old Road Campus Research Building, University of Oxford, Oxford, UK; †Acoustics Group, National Physical Laboratory, Teddington, UK; ‡Department of Physics and Astronomy, University College London, London, UK; and §Department of Mathematics, University College London, London, UK

(*Received* 17 *August* 2015; *revised* 22 *December* 2015; *in final form* 11 *January* 2016)

Abstract—There is increasing interest in the use of microbubble contrast agents for quantitative imaging applications such as perfusion and blood pressure measurement. The response of a microbubble to ultrasound excitation is, however, extremely sensitive to its size, the properties of its coating and the characteristics of the sound field and surrounding environment. Hence the results of microbubble characterization experiments can be significantly affected by experimental uncertainties, and this can limit their utility in predictive modelling. The aim of this study was to attempt to quantify these uncertainties and their influence upon measured microbubble characteristics. Estimates for the parameters characterizing the microbubble coating were obtained by fitting model data to numerical simulations of microbubble dynamics. The effect of uncertainty in different experimental parameters was gauged by modifying the relevant input values to the fitting process. The results indicate that even the minimum expected uncertainty in, for example, measurements of microbubble radius using conventional optical microscopy, leads to variations in the estimated coating parameters of ~20%. This should be taken into account in designing microbubble characterization experiments and in the use of data obtained from them. (E-mail: eleanor.stride@eng.ox.ac.uk) **© 2016 The Authors. Published by Elsevier Inc. on behalf of World Federation for Ultrasound in Medicine & Biology. This is an open access article under the CC BY license (http://creativecommons.org/licenses/by/4.0/).**

Key Words: **Microbubbles, Ultrasound contrast agent, Characterization, Modelling, Quantitative imaging, Uncertainty, Experimental error.**

INTRODUCTION

Suspensions of gas microbubbles stabilized by a surfactant, protein or polymer coating have been in clinical use as ultrasound contrast agents for more than two decades (Cosgrove 2006; Cosgrove and Lassau 2010). In recent years, they have also gained renewed interest for use in tissue perfusion and local blood pressure measurements for both diagnostic and treatment monitoring applications (Andersen and Jensen 2010; Hoyt et al. 2012; Sboros and Tang 2010). Compared with X-ray angiography or magnetic resonance imaging (MRI) techniques, quantitative ultrasound imaging offers considerable advantages in terms of convenience, cost and patient safety and, in many cases, superior specificity and sensitivity (Leen et al. 2002).

A significant limiting factor in developing more effective imaging algorithms, however, is the high degree of uncertainty in the relationship between microbubble concentration and the imaging signal (Tang et al. 2011). One source of this uncertainty is the difficulty in predicting the response of the microbubbles to ultrasound excitation. Much effort has been devoted to developing theoretical models to describe ultrasound-driven coated microbubble dynamics (Dejong et al. 1992; Church 1995; Marmottant et al. 2005; O'Brien et al. 2011; Stride 2008). Similarly, a number of highly sophisticated experimental techniques have been adapted specifically for microbubble characterization, including ultrahigh-speed video microscopy (Chin et al. 2003), flow cytometry (Tu et al. 2011) and high-frequency ultrasound measurements (Renaud et al. 2014).

Unfortunately, numerous studies have reported not only that there is considerable variability in microbubble

Address correspondence to: Eleanor Stride, Institute of Biomedical Engineering, University of Oxford, Old Road Campus Research Building, Oxford OX3 7 DQ, UK. E-mail: eleanor.stride@eng.ox.ac.uk

Data repository: The data from which the results presented in this paper are derived may be found at http://dx.doi.org/10.5287/bodleian:5RDr7BMKE.

response across a population (Postema et al. 2005; Rademeyer et al. 2015), but also that the microbubble response is extremely sensitive to the characteristics of the sound field (frequency, pressure, pulse duration), surrounding environment (liquid density, viscosity, surface tension and presence of any boundaries) and the microbubble itself (size, gas and coating properties). Hence the results obtained from microbubble characterization experiments are likely to be very sensitive to experimental uncertainties, and this inevitably limits their utility in predictive modelling. The aim of this study was to quantify these uncertainties and their influence upon measured microbubble characteristics.

METHODS

In the majority of experimental studies, measurement is made of either the time-varying volume or radius of the bubble, $R(t)$, and/or the pressure radiated as a result of these oscillations, $p_{\mathrm{rad}}(t)$, from which the radius can be derived (Sijl et al. 2008). These may be measured directly from individual bubbles or inferred from, for example, ultrasound attenuation or speed of sound in a microbubble suspension (Dejong et al. 1992). Given the high variability in bubble response, however, only the former are considered here.

Microbubble characteristics are determined through fitting of the experimental data to a selected theoretical model, which is typically of the form (Stride 2008):

$$R\ddot{R}+\frac{3}{2}\dot{R}^2=\frac{1}{\rho_L}\left[\left[p_0+\frac{2\sigma_0}{R_0}-p_v\right]\left[\frac{R_0}{R}\right]^{3\gamma}+p_v-\frac{2\sigma}{R}-f_s-\frac{4\mu_L\dot{R}}{R}-p_0+p_{ac}\right] \quad (1)$$

where R is the instantaneous bubble radius; the overdot denotes a time derivative, making $\dot{R}$ the velocity of the bubble wall and $\ddot{R}$ its acceleration. R_0 is the initial radius, f_s describes the influence of the microbubble coating, ρ_L is the density of the surrounding liquid, p_0 is the hydrostatic pressure, p_v is the vapor pressure inside the bubble, γ is the polytrophic constant (the gas is assumed to behave ideally), σ is the surface tension, with initial value σ_0, μ_L is the viscosity of the liquid (assumed to be incompressible and Newtonian) and p_{ac} is the pressure imposed by the ultrasound field.

Fitting may be achieved through: (i) linearization of the model to generate expressions for the amplitude and phase of microbubble oscillation, from which the unknown parameters can be determined by direct comparison with the experimental data; and (ii) optimization of the fit between the solution to the equation of motion and experimental data by varying the unknown parameters over iterative numerical solutions (Postema et al. 2004). Given the highly non-linear nature of microbubble behavior, the latter is usually the preferred method. For the purposes of this study, we used the constitutive equation for the coating used by Hoff et al. (2000):

$$R\ddot{R}+\frac{3}{2}\dot{R}^2=\frac{1}{\rho_L}\left[p_0\left[\frac{R_0}{R}\right]^{3\gamma}-\frac{12G_sd_sR_0^2(R-R_0)}{R^4}-\frac{12\mu_sd_s\dot{R}R_0^2}{R^4}-\frac{4\mu_L\dot{R}}{R}-p_0+p_{ac}\right] \quad (2)$$

The influence of the coating is described in terms of an infinitesimally thin linear viscoelastic shell characterized by its thickness, d_{s}, shear modulus, G_{s}, and shear viscosity μ_{s}. This selection was made in the interest of simplicity for illustration and to enable comparison with existing experimental data sets. It should, however, be noted that in the case of a surfactant-coated bubble, the concept of a shell "thickness" is somewhat misleading, as the elastic and viscous effects arise because of variations in surface molecular concentration. Hence the assignment of the value of 1 nm to d_{s} below does not indicate an accurate physical measure, and the quantities $G_s \times d_s$ and $\mu_s \times d_s$ could equally well be used as fitting parameters representing effective coating stiffness and viscosity, respectively (see Appendix).

To determine the effect of experimental uncertainty on the derived coating parameters, it is first necessary to estimate the magnitude of these uncertainties. There are several different sources: First, each measurement technique will have an associated uncertainty that will, in turn, affect each parameter used in the model. The initial bubble radius, R_0, is typically measured via bright-field optical microscopy and, thus, with a minimum uncertainty of ± 0.25 μm. Instantaneous bubble radius $R(t)$ measurements from high-speed video microscopy (Fig. 1) are subject to the same uncertainty. Added to this is the uncertainty due to the optical system, camera "pixel" resolution and frame rate, hence sampling frequency. In the case of laser scattering measurements, the uncertainty in $R(t)$ is approximately $\pm 0.5\%$ (Rademeyer et al. 2015). The quoted uncertainty for a calibrated hydrophone and, hence, for measurements of $p_{\mathrm{rad}}(t)$ and the incident field $p_{\mathrm{ac}}(t)$ varies between $\pm 5\%$ and 15% (Koukoulas et al. 2015). The hydrostatic pressure and liquid parameters are rarely reported as direct measurements in experiments, but assuming standard laboratory equipment, the uncertainty in these values can also be estimated. The parameters used for the simulations and the corresponding uncertainties are summarized in Table 1.

Sets of synthetic data were obtained by solving eqn (2) using a fourth-order Runge Kutta method

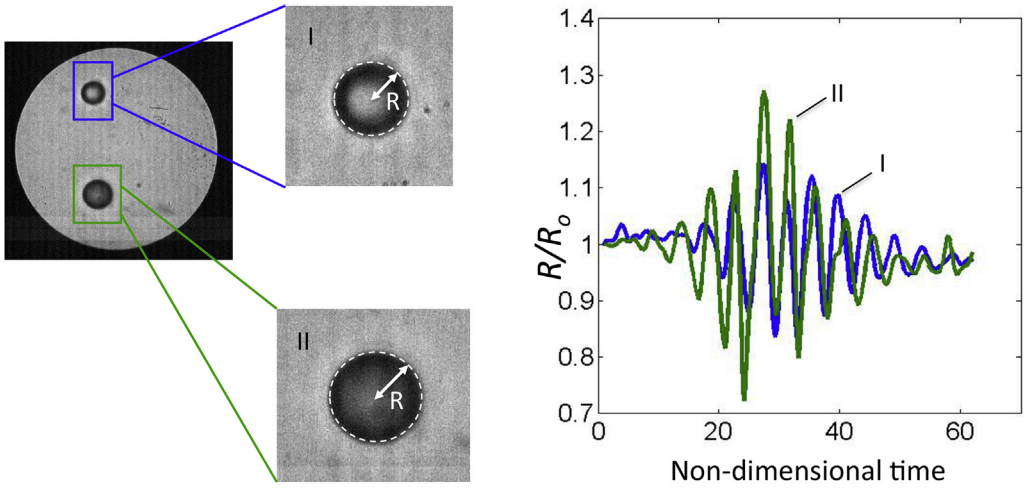

Fig. 1. Example of microbubble images captured by high-speed video microscopy (for experimental details, see Chetty et al. 2008). Left: Single video frame with magnified images of individual bubbles. Right: Corresponding radius–time ($R(t)$) curves for the bubbles obtained from the video sequence.

implemented in MATLAB (R2012, function ode45, The MathWorks, Natick, MA, USA). The equations were first recast and non-dimensionalized using the scheme [mass] = [p_0 R_0/ω^2], [length] = [R_0] and [time] = [$1/\omega$], where $\omega = 2\pi f$. It was assumed that the incident field was a simple sinusoidal plane wave $p_{ac} = p_a \sin(2\pi ft)$ of amplitude p_a and frequency f and that the field was constant across the bubble (*i.e.*, the wavelength was significantly larger than the bubble radius). For each of the conditions outlined in Table 1, model sets of data were generated for $R(t)$. These values were selected to be representative of published experimental studies utilizing high-speed video microscopy and/or laser scattering (*e.g.*, Chetty et al. 2008; Emmer et al. 2009; Rademeyer et al. 2015).

These sets were then "corrupted" by increasing or decreasing the values of $R(t)$ according to the relevant degree of uncertainty (between 1% and 20%). The effect on the calculated values of G_s and μ_s (d_s was assumed to be known) was assessed using the internal MATLAB lsqcurvefit function whereby eqn (2) was solved iteratively for varying values of G_s and μ_s until the squared difference between the solution and data set was minimized. The effect of uncertainty in the values of R_0, ρ_L, μ_L, p_0 and p_a was similarly determined by altering the corresponding input to eqn (2).

Table 1. Parameter values used in the simulations and associated estimated uncertainties

Parameter	Units	Value	Uncertainty	%
R_0	m	1.5 or 2.5 × 10^{-6}	0.25 × 10^{-6}	17 or 10
$R(t)$	m	Simulated	0.25 × 10^{-6}	n/a
p_A	Pa	1, 5 or 10 × 10^4	2.5, 5 or 25 × 10^3	5
F	Hz	2 × 10^6	n/a*	n/a
P_0	Pa	10^5	2500	2.5
μ_L	Pa·s	10^{-3}	10^{-5}	1
ρ_L	kg m^{-3}	10^3	5	0.5
Γ	—	1.4	n/a	n/a
d_s	m	$1e^{-9}$	n/a	n/a
G_s	Pa	10^8	n/a	n/a
μ_s	Pa·s	1.4	n/a	n/a

* The uncertainty in the driving frequency may be negligible because the recorded driving signal is typically used for data fitting (*e.g.*, Chetty et al. 2008), and the time bases of the driving and measured signals will be synchronized. As illustrated in Figure 3, however, this could be a further source of uncertainty if the driving pulse were also simulated based on an incorrect transducer calibration.

RESULTS

To validate the fitting technique, the lsqcurvefit function was first run on the "true" data for each set of conditions, and it was confirmed that this yielded the original values of G_s and μ_s with <1% intrinsic fitting error. In all cases, the termination criterion for the fitting process was that a local minimum corresponding to the optimal solution had been found. Figures 2–4 illustrate the effect upon the fitted values of G_s and μ_s of uncertainty in the microbubble radius, incident ultrasound pressure and frequency, liquid physical properties and hydrostatic pressure measurements. Tables 2 and 3 summaries the effect of different values of uncertainty in the measurements of $R(t)$ (with the larger uncertainty corresponding to high-speed video microscopy and the smaller to laser scattering) upon the fitted values of G_s and μ_s, respectively, for different initial bubble sizes and acoustic pressures.

DISCUSSION

The data in Figure 2 indicate that uncertainty in the measurements of R_0 and $R(t)$ can have a significant effect upon the estimated values of G_s and μ_s. Similarly, Figure 3 illustrates that uncertainty in f and p_a can also

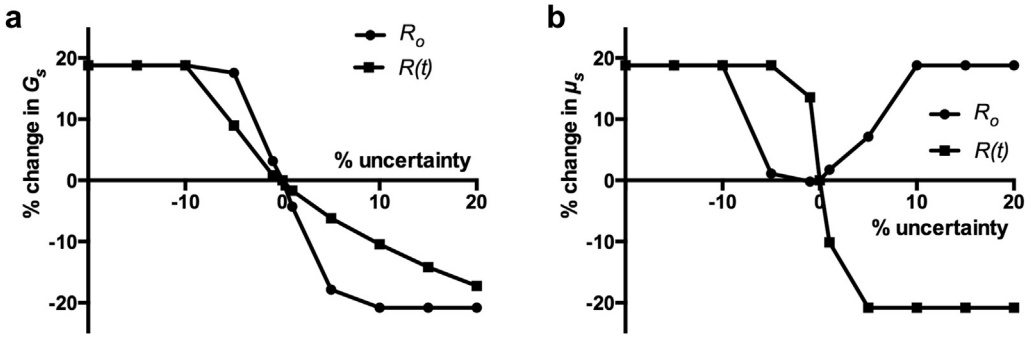

Fig. 2. Effect of uncertainty in the measurements of microbubble radius (initial and time dependent) upon the fitted values of (a) G_s and (b) μ_s. The other simulation parameters were kept constant, as indicated in Table 1.

lead to considerable variation in the fitted coating parameters. Tables 2 and 3 indicate that the effect is pronounced at lower pressures when the uncertainty corresponds to a significant proportion of the measured radial excursion. This is of particular importance because coating parameters are often derived from measurements at low acoustic driving pressures and/or off-resonance to avoid regimes in which the assumptions underpinning theoretical models are invalid, to avoid shape oscillations and/or microbubble destruction. The estimated uncertainties in the properties of the surrounding liquid and atmospheric pressure are proportionally smaller (Table 1), and their effect upon G_s and μ_s is less significant (Fig. 4).

It is likely that the uncertainties for pressure and radius measurements listed in Table 1 are in fact underestimates. Suboptimal focusing and/or translation of a microbubble during an experiment will increase the uncertainty in $R(t)$, as will imperfections in the optical system. Similarly noise caused by propagation effects and the particular electronics used for acoustic measurements may add to the uncertainty in p_a and/or $p_{rad}(t)$. In addition, there are a number of other factors that should be considered. In many cases it is necessary to physically confine microbubbles to perform measurements upon them. This has been shown theoretically and experimentally to influence the amplitude of oscillation (Garbin et al. 2007a) and means that $R(t)$ will depend upon the plane of observation (Vos et al. 2007). Furthermore the assumption of spherical behavior underlying eqn (2) may be invalidated in the case of a confined bubble.

The selection of the value of γ is also worthy of mention. Previous studies have treated the expansion and compression of the gas inside the bubble as either isothermal ($\gamma = 1$) or adiabatic ($\gamma = 1.4$ for air). The argument for the latter is that on the time and length scales associated with microbubble oscillations relevant for ultrasound imaging/therapy, heat transfer in aqueous media will be negligible (hence the absence of thermal damping terms in eqn 1). To examine the influence of this assumption, further simulations were conducted assuming isothermal behavior in generating the model data, but adiabatic behavior for fitting and *vice versa*. In the first case, values for G_s and μ_s of 119 MPa and 1.16 Pa·s were obtained, and in the second, 79 MPa and 0.99 Pa·s, indicating that this is in fact an important consideration, particularly because the composition of the gas inside the microbubbles may change over time (Kwan and Borden 2010).

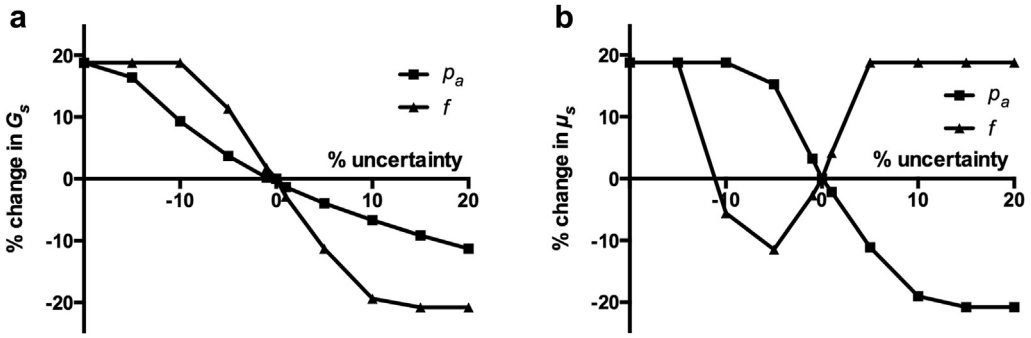

Fig. 3. Effect of uncertainty in the incident pressure and frequency upon the fitted values of (a) G_s and (b) μ_s. The other simulation parameters were kept constant, as indicated in Table 1.

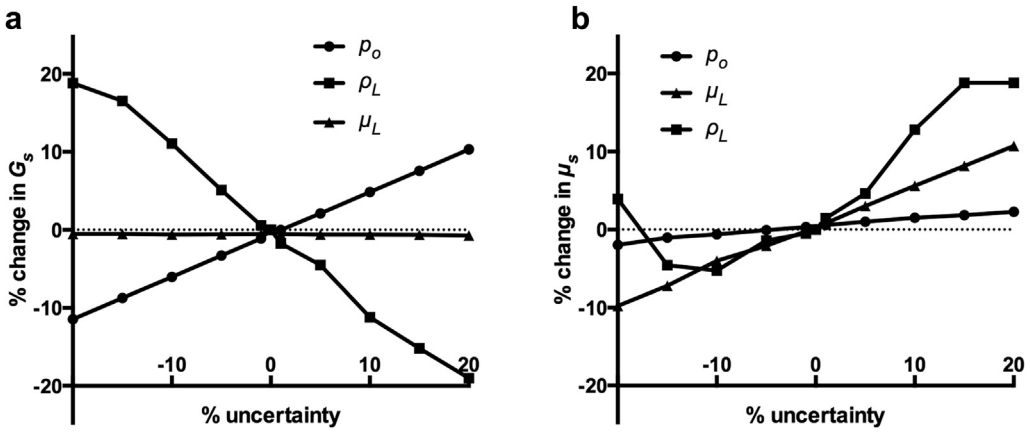

Fig. 4. Effect of uncertainty in the surrounding liquid parameters upon the fitted values of (a) G_s and (b) μ_s. The other simulation parameters were kept constant, as indicated in Table 1.

Alternative constitutive equations suitable for larger-amplitude oscillations (*e.g.,* Marmottant et al. 2005), including time-dependent effects such as lipid shedding (O'Brien et al. 2011) and/or translational motion (Garbin et al. 2007b), can be substituted for eqn (2), but these too assume spherical behavior. Moreover, increasing the complexity of the model increases the number of parameters that need to be accurately measured and/or obtained through fitting. It has been reported previously (Harfield et al. 2013) that there will be a unique pair of parameters corresponding to the best fit between equations of the form of (2) and $R(t)$ data (see Appendix), but this is not the case for more sophisticated models.

Improving the accuracy with which experimental parameters are measured through rigorous calibration of acoustic equipment and characterization of the surrounding liquid can help to mitigate these uncertainties. Similarly, the use of systems enabling isolated microbubble measurements (Fury et al. 2014; Garbin et al. 2006; Rademeyer et al. 2015) is to be preferred, although bubble–bubble and bubble–wall interactions will still inevitably occur *in vivo*. Previous work has also indicated that the use of fluorescence microscopy (Gelderblom et al. 2012) offers superior precision in the measurement of $R(t)$, comparable to that of laser scattering, but still enabling direct visualization.

In terms of the implications for applications requiring accurate quantification of microbubble signals, a 20% error in the coating parameter values would correspond to a ~0.1-MHz shift in the microbubble resonance frequency (1.77 MHz from the linearized version of eqn [2]) (Hoff et al. 2000). This would be approximately equivalent to the shift produced by a 30% change in the hydrostatic pressure and, thus, would have negative consequences, for example, for blood pressure sensing applications. Similarly, it could lead to significant errors in estimates of microbubble concentration. In both of these applications, however, the ensemble response of a microbubble population is measured, and hence, an even more significant challenge is likely to be posed by interbubble variability and variations in size distribution and/or coating properties over time. Moreover, *in vivo* there will be numerous additional factors influencing microbubble dynamics. These factors include interactions between microbubbles and between microbubbles and blood vessel walls (Chen et al. 2011; Martynov et al. 2011), absorption of blood gases (Kwan and Borden

Table 2. Effect of uncertainty in the measurements of the time-dependent microbubble radius upon the fitted value of G_s

		Uncertainty in $R(t)$			
		1%	−1%	17%	−17%
R_0 (μm)	p_a (kPa)	Fitted value of G_s (MPa)			
1.50	10	99	99	99	99
1.50	50	98	101	84	119
1.50	100	99	99	95	109
2.50	10	100	97	106	79
2.50	50	99	99	98	99
2.50	100	99	98	102	95

Table 3. Effect of uncertainty in the measurements of the time-dependent microbubble radius upon the fitted value of μ_s

		Uncertainty in $R(t)$			
		1%	−1%	17%	−17%
R_0 (μm)	p_a (kPa)	Fitted value of μ_s (Pa·s)			
1.50	10	0.99	0.99	1.0	1.0
1.50	50	0.90	1.14	0.79	1.19
1.50	100	0.92	0.99	0.82	1.18
2.50	10	0.79	1.19	0.79	1.19
2.50	50	0.98	0.99	0.95	1.02
2.50	100	0.99	0.99	0.95	0.99

2010), attenuation and non-linear propagation of the incident acoustic field. Investigation of these parameters is outside the scope of the present study, which is focused on the *in vitro* characterization of single bubbles. Clearly, however, these factors cannot be neglected when considering the more general case of uncertainty associated with quantitative ultrasound contrast imaging techniques.

CONCLUSIONS

The results of the study indicate that it is important to perform an uncertainty analysis when deriving microbubble characteristics by fitting theoretical models to experimental data. Without this, the utility of theoretical modeling in developing algorithms for quantitative applications is limited. It is similarly important to design experimental measurement protocols to minimize and enable quantification of uncertainty.

Acknowledgments—The authors acknowledge funding through the National Physical Laboratory Strategic Research fund (Project 114248) and the Engineering and Physical Sciences Research Council (Grant EP/I021795/1).

REFERENCES

Andersen KS, Jensen JA. Non-invasive estimation of blood pressure using ultrasound contrast agents. Phys Proc 2010;3:245–253.

Chen H, Brayman AA, Kreider W, Bailey MR, Matula TJ. Observations of translation and jetting of ultrasound-activated microbubbles in mesenteric microvessels. Ultrasound Med Biol 2011;37:2139–2148.

Chetty K, Stride E, Sennoga CA, Hajnal JV, Eckersley RJ. High-speed optical observations and simulation results of SonoVue microbubbles at low-pressure insonation. IEEE Trans Ultrason Ferroelectr Freq Control 2008;55:1333–1342.

Chin CT, Lancee C, Borsboom J, Mastik F, Frijlink ME, de Jong N, Versluis M, Lohse D. Brandaris 128: A digital 25 million frames per second camera with 128 highly sensitive frames. Rev Sci Instrum 2003;74:5026–5034.

Church CC. The Effects of an Elastic Solid-surface layer on the radial pulsations of gas-bubbles. J Acoust Soc Am 1995;97:1510–1521.

Cosgrove D. Ultrasound contrast agents: An overview. Eur J Radiol 2006;60:324–330.

Cosgrove D, Lassau N. Imaging of perfusion using ultrasound. Eur J Nucl Med Mol Imaging 2010;37:65–85.

Dejong N, Hoff L, Skotland T, Bom N. Absorption and scatter of encapsulated gas filled microspheres: Theoretical considerations and some measurements. Ultrasonics 1992;30:95–103.

Emmer M, Vos HJ, Goertz DE, van Wamel A, Versluis M, de Jong N. Pressure-dependent attenuation and scattering of phospholipid-coated microbubbles at low acoustic pressures. Ultrasound Med Biol 2009;35:102–111.

Fury C, Jones PH, Memoli G. Multiscale manipulation of microbubbles employing simultaneous optical and acoustical trapping. Proc SPIE 2014;9164.

Garbin V, Cojoc D, Ferrari E, Di Fabrizio E, Overvelde MLJ, van der Meer SM, de Jong N, Lohse D, Versluis M. Changes in microbubble dynamics near a boundary revealed by combined optical micromanipulation and high-speed imaging. Appl Phys Lett 2007a;90:114103.

Garbin V, Dollet B, Overvelde MLJ, de Jong N, Lohse D, Versluis M, Cojoc D, Ferrari E, Di Fabrizio E. Coupled dynamics of an isolated UCA microbubble pair. Proc IEEE Ultrason Symp 2007b;757–760.

Garbin V, Ferrari E, Cojoc D, Di Fabrizio E, Overvelde MLJ, van der Meer SM, Versluis M. Optical trapping of ultrasound contrast agent microbubbles. Proc IEEE Ultrason Symp 2006;513–516.

Gelderblom EC, Vos HJ, Mastik F, Faez T, Luan Y, Kokhuis TJA, van der Steen AFW, Lohse D, de Jong N, Versluis M. Brandaris 128 ultra-high-speed imaging facility: 10 y of operation, updates, and enhanced features. Rev Sci Instrum 2012;83:103706.

Harfield CJ, Ovenden NC, Memoli G, Jones PH, Stride EPJ. Theoretical characterisation of the radial and translational motion of coated microbubbles under acoustic excitation. In: Proceedings, 11th Anglo-French Physical Acoustics Conference (AFPAC 2012). *J Phys Conf Ser* 2013;457:012001.

Hoff L, Sontum PC, Hovem JM. Oscillations of polymeric microbubbles: Effect of the encapsulating shell. J Acoust Soc Am 2000;107:2272–2280.

Hoyt K, Sorace A, Saini R. Quantitative mapping of tumor vascularity using volumetric contrast-enhanced ultrasound. Invest Radiol 2012;47:167–174.

Koukoulas T, Piper B, Rajagopal S, Robinson SP, Zeqiri B. Calibration of acoustical devices through particle motion measurements in air and water using laser based methods. In: Proceedings, 22nd International Congress on Sound and Vibration, Florence, Italy, 12–16 July 2015.

Kwan JJ, Borden MA. Microbubble dissolution in a multigas environment. Langmuir 2010;26:6542–6548.

Leen E, Angerson WJ, Yarmenitis S, Bongartz G, Blomley M, Del Maschio A, Summaria V, Maresca G, Pezzoli C, Llull JB. Multicentre clinical study evaluating the efficacy of SonoVue (TM) (BR1), a new ultrasound contrast agent in Doppler investigation of focal hepatic lesions. Eur J Radiol 2002;41:200–206.

Marmottant P, van der Meer S, Emmer M, Versluis M, de Jong N, Hilgenfeldt S, Lohse D. A model for large amplitude oscillations of coated bubbles accounting for buckling and rupture. J Acoust Soc Am 2005;118:3499–3505.

Martynov S, Kostson E, Saffari N, Stride E. Forced vibrations of a bubble in a liquid-filled elastic vessel. J Acoust Soc Am 2011;130:2700–2708.

O'Brien JP, Ovenden N, Stride E. Accounting for the stability of microbubbles to multi-pulse excitation using a lipid-shedding model. J Acoust Soc Am 2011;130:EL180–EL185.

Postema M, Bouakaz A, Versluis M, de Jong N. Ultrasound-induced gas release from contrast agent microbubbles. IEEE Trans Ultrason Ferroelectr Freq Control 2005;52:1035–1041.

Postema M, Van Wamel A, Lancee CT, De Jong N. Ultrasound-induced encapsulated microbubble phenomena. Ultrasound Med Biol 2004;30:827–840.

Rademeyer P, Carugo D, Lee JY, Stride E. Microfluidic system for high throughput characterisation of echogenic particles. Lab Chip 2015;15:417–428.

Renaud G, Bosch JG, Van Der Steen AFW, De Jong N. Low-amplitude non-linear volume vibrations of single microbubbles measured with an "acoustical camera." Ultrasound Med Biol 2014;40:1282–1295.

Sboros V, Tang MX. The assessment of microvascular flow and tissue perfusion using ultrasound imaging. Proc Inst Mech Eng Part H 2010;224:273–290.

Sijl J, Gaud E, Frinking PJ, Arditi M, de Jong N, Lohse D, Versluis M. Acoustic characterization of single ultrasound contrast agent microbubbles. J Acoust Soc Am 2008;124:4091–4097.

Stride E. The influence of surface adsorption on microbubble dynamics. Philos Trans R Soc A 2008;366:2103–2115.

Tang MX, Mulvana H, Gauthier T, Lim AKP, Cosgrove DO, Eckersley RJ, Stride E. Quantitative contrast-enhanced ultrasound imaging: A review of sources of variability. Interface Focus 2011;1:520–539.

Tu J, Swalwell JE, Giraud D, Cui WC, Chen WZ, Matula TJ. Microbubble sizing and shell characterization using flow cytometry. IEEE Trans Ultrason Ferroelectr Freq Control 2011;58:955–963.

Vos HJ, Versluis M, de Jong N. Orthogonal observations of vibrating microbubbles. Proc IEEE Ultrason Symp 2007;765–768.

APPENDIX

To be useful for characterization of the microbubble coating, it is essential that a unique set of parameters can be derived by fitting experimental data to the output from the model.

The unknowns in eqn (2) are μ_s, d_s and G_s, which can be treated as a pair of lumped parameters $G_s d_s = v$ and $\mu_s d_s = u$ (d_s can either be measured independently or equivalent material properties can be inferred from surface chemistry models) (Stride 2008). It is assumed that these values are constant over a single oscillation. To prove uniqueness, it must be shown that different sets of v and u cannot produce the same $R(t)$ curve. If the opposite is assumed, then rewriting eqn (2) where the coating is characterized by either v_1,u_1 or v_2,u_2 gives

$$F\left(\ddot{R},\dot{R},R\right) = -\frac{12\,R_0^2\dot{R}}{\rho_L R^5}u_1 - \frac{12\,R_0^2}{\rho_L R^4}\left(1-\frac{R_0}{R}\right)v_1 \tag{A1a}$$

$$F\left(\ddot{R},\dot{R},R\right) = -\frac{12\,R_0^2\dot{R}}{\rho_L R^5}u_2 - \frac{12\,R_0^2}{\rho_L R^4}\left(1-\frac{R_0}{R}\right)v_2 \tag{A1b}$$

where $F(\ddot{R},\dot{R},R)$ contains all the terms in eqn (2) that do not contain either parameter u_i or v_i, thus indicating that the right-hand sides of eqn (A1a) and (A1b) must be equal. Equating and rearranging give

$$\dot{R} + \frac{R(v_1-v_2)}{(u_1-u_2)} = \frac{R_0(v_1-v_2)}{(u_1-u_2)} \tag{A2}$$

Letting $(v_1 - v_2)/(u_1 - u_2) = \beta$ and solving, we obtain for an arbitrary constant C the solution

$$R(t) = R_0 + Ce^{-\beta t} \tag{A3}$$

Thus, eqn (A3) represents the only type of bubble behavior where bubbles with different sets of coating parameters may be indistinguishable from one another. Moreover, as β is always real, we can conclude that for an oscillating bubble governed by eqn (2), only a unique set of u and v can replicate the observed $R(t)$ curve.